

Quantifying the microstructural inhomogeneity of $\text{Zr}_{46}\text{Cu}_{46}\text{Al}_8$ metallic glasses based on change ratio of polyhedral volume

S.D. Feng^{a,b,*}, K.C. Chan^{a,*}, R.P. Liu^b

^a*Advanced Manufacturing Technology Research Centre, Department of Industrial and
Systems Engineering, The Hong Kong Polytechnic University, Hong Kong.*

^b*State Key Laboratory of Metastable Materials Science and Technology, Yanshan
University, Qinhuangdao 066004, China*

Submitted to Journal of Alloys and Compounds

* Corresponding author:

Dr. S.D. Feng

E-mail: shidong.feng@polyu.edu.hk

Dr. K.C. Chan

E-mail: kc.chan@polyu.edu.hk

Abstract

The microstructural inhomogeneity of $\text{Zr}_{46}\text{Cu}_{46}\text{Al}_8$ metallic glasses is investigated quantitatively by molecular dynamics simulation. A parameter, the change ratio of polyhedral volume, is used to characterize the microstructural inhomogeneity in metallic glasses. Based on identifying the polyhedral volume expansion and contraction around each atom, the microstructural heterogeneity of metallic glasses can be revealed and quantified. The relation between the redistribution of the free volume and production or annihilation of defects has been established. By molecular dynamics simulations of dynamic mechanical tests, the distribution of the change ratio of polyhedral volume is correlated to dynamic heterogeneities in metallic glasses at the atomic level. Our work opens a new technologically avenue towards the characterization of microstructural inhomogeneity that affects the thermodynamics, dynamics and deformation in metallic glasses.

Keywords: *Metallic glass; Microstructural inhomogeneity; Free volume; Molecular dynamics simulation*

1. Introduction

In the macrostructural view, metallic glasses (MGs) all appear completely amorphous. While in the microstructural view, because of inherited disordered structure of liquids, MGs are characterized by the heterogeneous atomic configuration [1], resulting in outstanding properties not found in crystalline metals [2-7]. Through numerous ways, scientists have proved the existence of the microstructural

heterogeneity in MGs. For example, through ultrasound-accelerated crystallization in Pd-based MGs, Ichitsubo et al. inferred that the typical features in fragile MGs are composed of strongly bonded regions and weakly bonded surroundings [8]. Using molecular dynamics simulation and nanobeam electron diffraction, Hirata et al. reported that individual atomic clusters and their assemblies can be experimentally observed [9]. By small angle X-ray scattering, Zhang et al. found the range of medium length scales over which structural rearrangements occur should be the structural origin of the heterogeneous dynamics of MGs [10]. These are clearly related to the heterogeneous microstructure of MGs, in which the local structure varies significantly on the nanometer scale.

To study heterogeneous microstructure of MGs at the atomic scale, several structural models have been proposed, such as coordination number, configurational potential energy [11], topological local order [12], and so on. These pioneering models all aim at different analysis in MGs, but they have some limitations. For example, the coordination number can reflect the packing density of local structures, but is difficult to provide the geometric symmetry of these structures. Configurational potential energy could reflect the relative stability of different MGs states, but is difficult to use to compare different compositions. Icosahedral clusters cannot only reflect microstructural heterogeneity, but also establish good relations with deformation and dynamic. However, in some MGs, icosahedral clusters are absent. As a result, it is still disputable as how each atom independently affects the heterogeneous microstructure of MGs. Therefore, a more effective model for

microstructural heterogeneity needs be proposed.

The definition of free volume is the extra volume relative to one ideal disordered atomic state of the largest density. In 1959, Cohen and Turnbull [13], using the free-volume concept, predicted that MGs can be prepared when liquid is cooled sufficiently. Then, free volume was extended by Spaepen to explain plastic deformation in MGs [14]. In Spaepen's model, if atoms move to smaller positions from the original locations under applied stress, free volume is created. Later, Argon found that free volume existed in a group of atoms, which were sufficient to carry out local shear transformation [15]. The free-volume model, combined with energy, can be useful for describing the structure, dynamics, thermodynamics and deformation [16]. Recently, Wang et al. found that homogeneous spatial distributions of free volume [17] and gradient of free volume distribution in MGs [18] can dramatically change mechanical properties. Meanwhile, orientation and statistical distribution of free volumes can affect the mechanical responses of spinodal decomposed MG composites [19]. Ding et al. introduced 'flexibility volume' as a universal indicator, which builds a bridge between the structure and properties of MGs [20]. There are descriptions and a number of constitutive models of volumetric change in deformation of MGs [21-24]. Definitely, there are some pitfalls for using "free volume" theory to describe MGs [1, 25]. So while it can be used for phenomenological studies, its limitations should be realized. For example, the free volume can't be well determined quantitatively, and doesn't contain information about the topological symmetry and chemically ordered local environment in itself [26].

Studying the volumetric change in microstructural inhomogeneity quantitatively, should be very meaningful as the volume is sensitive to small changes in the atomic configurations [27]. Free volume is a global concept and defines an average value. In contrast, the present paper deals with a local point of view. Various authors introduced the concept of “pseudo-defects” in amorphous materials. For example, Granato defined the interstitialcy theory [28, 29], while Perez introduced the concept of quasi-point defects [30], which corresponds to zones where the packing may be higher or lower than the average. The quasi-point defects theory can be adopted to predict the atomic mobility and mechanical properties of MGs [31, 32]. In addition, Liu et al. claimed that both soft and hard zones exist in the MGs [33]. Free volume change has been investigated by density measurement [34], positron annihilation [35], enthalpy measurements [36], and so on. These methods have demonstrated that during thermal annealing of MGs, annihilation of free volume is less than 0.5% approximately. Meanwhile, because of inherent limitations in the spatial resolutions, the experimental methods characterizing the free volume change cannot reach the atomic scale. Therefore, atomic free volume change is not easy to measure accurately, and hence is not very effective to use for predicting properties. Determining precisely the subtle changes in free volume has been a challenge at the atomic scale.

To investigate the evolution of free volumes at the atomic level, molecular dynamics (MD) simulation of $\text{Zr}_{46}\text{Cu}_{46}\text{Al}_8$ MGs was employed. There are also recent literature (MD and experimental) highlighting the specific role of free volume (via Voronoi volume) in the microstructural and mechanical properties of MGs [37, 38].

Compared to Zr-Cu MGs, the alloying of Al into Zr-Cu can promote the adding of icosahedral clusters and affect mechanical properties of MGs distinctly [1, 39]. In the present study, we studied the microstructural inhomogeneity of $\text{Zr}_{46}\text{Cu}_{46}\text{Al}_8$ MGs by the volume change ratio of Voronoi polyhedra, whose faces bisect connecting the central atom to its neighboring atoms at right angles [40]. The polyhedra can be characterised by the Voronoi index $[n_3, n_4, n_5, n_6]$, where n_i denotes the number of i -edged faces of the Voronoi polyhedra. With this mind, each atom of a Voronoi polyhedron can share the effective space with all nearest neighbors. Based on this, the change ratio of polyhedral volume can be identified and analyzed in terms of the number of polyhedra, their volume, and their shape. The available space surrounding each atom, that is necessary for atomic motion, is also clear. In search of a realistic picture of microstructural inhomogeneity, the correlation between the "free" character of the free volume and microstructural inhomogeneity in MGs is discussed.

2. Model and simulation details

Molecular dynamics simulations were performed in LAMMPS, based on embedded atom potential parameterized by Cheng et al., which has been successfully employed to resolve the atomic structure of ternary CuZrAl MGs [41, 42]. The $\text{Zr}_{46}\text{Cu}_{46}\text{Al}_8$ model, containing approximately 100,000 atoms, was equilibrated for 5 ns at 2000 K under periodic boundary conditions. Then it was cooled to 100 K at 1 K ps^{-1} and 0 Pa under NPT ensemble. Molecular dynamics simulations of dynamic mechanical spectroscopy (MD-DMS) were employed to obtain dynamic deformation

information [43]. This method applied a sinusoidal strain $\varepsilon = \varepsilon_A \sin \omega t$, where ω is the angular frequency and ε_A is the amplitude, fixed within the linear elastic regime. The resultant stress was fitted as $\sigma = \sigma_A \sin (\omega t + \delta)$, where δ is the phase difference between stress and strain. Storage (E') and loss (E'') modulus values were calculated as $E' = \sigma_A / \varepsilon_A \cos(\delta)$ and $E'' = \sigma_A / \varepsilon_A \sin(\delta)$, respectively. The free volume (V_f) can be defined as the Voronoi volume less the atomic core volume, as follows [44].

$$V_f = V_i^{voro} - V_i^{atom} \quad (1)$$

Where V_i^{voro} represents the Voronoi volume of the i th atom, and V_i^{atom} represents the core volume of the i th atom. Note that due to different atomic radii, the Voronoi method for calculating the volume should be weighted according to the atomic size differences. Since V_i^{atom} is generally a constant, it is reasonable to substitute V_i^{voro} for the free volume V_f . In this paper, V_i^{voro} will be used to replace the free volume.

3. Results and discussion

Because the microstructure of MGs combines two aspects: a high-density packing fraction and a concentration of the free volume. The latter, the concentration of the free volume, is closely related to the atomic structure and atomic mobility. For example, MGs are stable kinetically below T_g with the absence of free volume. However, upon reheating at different temperatures below T_g , some of the liquid's free volume is activated. **Figure 1** shows the distributions of the contributing volume of Zr-centered, Cu-centered and Al-centered polyhedra with reheating at 550 K, 650 K and 750 K ($T_g = 750$ K). The contributing volume of one type of polyhedron can be

defined as the number of the polyhedron multiplied by the average volume of the polyhedron. As shown in [Figure 1](#), with the increasing temperature, the contributing volumes of the Zr-centered polyhedra with index $\langle 0, 1, 10, 4 \rangle$, $\langle 0, 2, 8, 5 \rangle$ and $\langle 0, 1, 10, 5 \rangle$ all decreased. Similar phenomenon is observed for those of the Cu-centered polyhedra with index $\langle 0, 2, 8, 1 \rangle$, $\langle 0, 2, 8, 2 \rangle$, $\langle 0, 0, 12, 0 \rangle$ and Al-centered polyhedra with index $\langle 0, 0, 12, 0 \rangle$, $\langle 0, 1, 10, 2 \rangle$. With the increasing temperature, although the volume of these polyhedra may slightly increase, there is an obvious reduction in their number due to the destruction of symmetry during the reheating process. Based on the above, the contributing volumes of these highly symmetrical polyhedra are found to be reduced. However, with the increasing temperature, the contributing volumes of the Al-centered polyhedra with index $\langle 0, 3, 6, 3 \rangle$, $\langle 0, 3, 6, 4 \rangle$, $\langle 0, 2, 8, 1 \rangle$ and $\langle 0, 2, 8, 2 \rangle$ all increased. Meanwhile, the number of the Zr-centered, Cu-centered and Al-centered fragmented polyhedra increased significantly with increasing temperature. The fragmented polyhedra are composed of all kinds of low-content polyhedra, that possess low symmetry and high entropy [\[45\]](#). Their corresponding clusters are also more energetic and mobile. For example, the contributing volume of Al-centered fragmented polyhedra increased from 34677 \AA^3 in the 550 K state to 38950 \AA^3 in the 750 K state. On the other hand, if normalized by the entire model volume ($1,728,000 \text{ \AA}^3$), the volume changes are less than 0.25%, which explains the difficulties in accurate measuring experimentally. While the contributing volume in the some polyhedra increases, the contributing volume of other polyhedra has a decreasing trend. Based on the differences of the contributing

volume of polyhedra, the microstructural heterogeneity of MGs is revealed.

Although the distributions of contributing volume of polyhedra are consistent with free-volume theory, little attention has been paid to the forming process of the free volume at the atomic scale. During reheating, the atomic motion leads to redistribution of the volume around the atoms. As shown in [Figure 2](#), compared to the quenched state, the total volume of the model reheated at 650 K increased, as indicated by dashed arrows. In detail, atoms A and A' correspond to the volume expansion, while atoms B and B' correspond to the volume contraction. By identifying the volume expansion and contraction around these atoms, the microstructural heterogeneity of MGs can be quantified.

Based on the above, the microstructural heterogeneity of MGs is quantified by a parameter C_i , defined as the change ratio of the polyhedral volume less the change ratio of the volume of the model.

$$C_i = \frac{V_{pi}^1 - V_{pi}^0}{V_{pi}^0} - \frac{V_M^1 - V_M^0}{V_M^0} \quad (2)$$

where V_{pi}^0 represents the volume of polyhedra i before reheating, while V_{pi}^1 represents that after reheating. V_M^0 represents the volume of model before reheating, while V_M^1 represents that after reheating.

As shown in [Figure 3](#), C_i can present inhomogeneity very well. Compared to the model reheated from 450 K to 500 K with the model reheated from 700 K to 750 K, it is found that with the increase of temperature, the change of C_i becomes more apparent. A clear effect of structural relaxation is visible in the random volume distributions of the atoms at different temperatures. Structural relaxation induced by

temperature treatment, leads to different free volume, which comes from the break and re-formation of the atomic bonds. This means that the contribution values of the polyhedra become more and more uneven at higher temperature. Accompanied by increasing temperatures, the volume changes reach a certain degree, and it needs less energy to move the atoms. Therefore, redistribution of the free volume leads to the production or annihilation of defects, forming microstructural heterogeneity. In previous work, the number of quasi-nearest atoms, N_Q , focusing on the cluster defects, can better reflect the correlation between the local structure and the defects [46]. Two atoms as a pair of quasi-nearest atoms should meet all the following three conditions: (I) they share a common nearest neighbor; (II) they are adjacent to each other, defined by that their corresponding Voronoi faces of the Voronoi polyhedron, centered by their common nearest neighbor, share an edge; (III) they are not the nearest neighbors of each other [47].

To quantify the correlation between C_i and N_Q for each element, the atoms are sorted by their N_Q from low to high. Next, these atoms are divided into n_g groups, and each group contains n_a atoms. The average C_i ($\langle C_i \rangle$) and N_Q ($\langle N_Q \rangle$) are calculated for each group. **Figure 4(a)** shows $\langle C_i \rangle$ exhibits a linear relation with $\langle N_Q \rangle$ under $n_a = 200$ for Zr, Cu and Al. To quantify the linear relation coefficient, the Pearson correlation coefficient K is used, as follows.

$$\text{-----} \tag{3}$$

where $E(X)$ and $E(Y)$ are the average values of variables X and Y , and $D(X)$ and $D(Y)$ are the standard deviations of variables X and Y . $K = 1$ or $K = -1$ represents maximum

correlation, while $K = 0$ indicates no correlation. **Figure 4(b)** shows the Pearson correlation coefficient K between C_i and N_Q as a function of n_a . It can be seen that K for both Cu and Al is higher than that of Zr. This fact suggests that microstructural heterogeneity depends the element. When n_a increases, K increases rapidly. When n_a is more than 20, K reaches 0.6~0.8, suggesting the linear relation is becoming strong. When n_a is more than 200, K is close to 1, which suggests that the correlation is the strongest. These prove that C_i and N_Q are closely correlated. Meanwhile, C_i can provide a more direct description of microstructural heterogeneity.

In order to verify the practicability of the parameter C_i in the structure-property relationship in MGs, dynamic mechanical tests were performed in MD simulations. **Figure 5** displays the normalized storage modulus E'/E_u and normalized loss modulus E''/E_u as functions of $\langle C_i \rangle$ for Al centered polyhedra at different temperatures. Here, E_u is the non-relaxed modulus, which is assumed to be E' at 100 K. The frequency was set to 100 GHz. Because of inherent limitations of MD method, the time and size scale in MD simulation is much shorter than the experimental time scale. So E'/E_u computed here is higher than that reported on dynamic mechanical analysis experiment. But the results are still of significance in understanding the phenomenon [43, 46, 48, 49]. For example, Qiao et al. found that the stress-driven event involves fast event as the local atomic rearrangement, while the thermally activated event is the percolation of the fast event involving a significant contribution from the atomic diffusion, which is consistent with the experimental observations [49]. And atomistic simulations can demonstrate the interplay between fast and slow event

and display similar results with experimental observations. Yu et al. pointed that the findings of the molecular dynamics simulation of dynamical mechanical spectroscopy can be compared with experiments and have implications in controlling storage (E') and loss (E'') modulus in MGs [43].

As shown in **Figure 5**, $\langle C_i \rangle$ exhibits a linear relation with the normalized storage modulus E'/Eu , while there is a sine relationship between $\langle C_i \rangle$ and E''/Eu . The asymmetrical peaks of normalized loss modulus E''/Eu corresponding to α relaxations, signaling the transition from glassy to supercooled liquid states [43]. With the increase of $\langle C_i \rangle$, the normalized storage modulus E'/Eu becomes lower. Because $\langle C_i \rangle$ is defined as the change ratio of the polyhedral volume less the change ratio of the volume of the model after reheating. Through this definition, $\langle C_i \rangle$ is zero if the change ratio of the polyhedral volume is equal to the change ratio of the volume of the model after reheating, corresponding the change homogeneity of polyhedra. More positive values of C_{ij} indicate more expansive polyhedral volumes compared to the model, whereas negative values of C_{ij} indicate contraction of polyhedral volumes compared to the model. After reheating, these atoms in the expanded regions of polyhedra are arranged loosely and their structures are not dense, which makes the atomic clusters be unable to withstand higher resistance. This explains why the larger the $\langle C_i \rangle$ value is, the smaller E'/Eu is. While in the negative regions of $\langle C_i \rangle$ values, the contraction of polyhedral volumes results in atoms being denser. So, these clusters are not easy to move, leading to the larger E'/Eu . These results are consistent with related experiments [50-53]. The above results indicate that the $\langle C_i \rangle$ has a strong

correlation with the normalized storage modulus E'/Eu and normalized loss modulus E''/Eu . Through adjusting the distribution of $\langle C_i \rangle$, dynamic heterogeneities in MGs can be changed.

4. Conclusion

Based on MD simulations, the microstructural inhomogeneity characterized by C_i in $Zr_{46}Cu_{46}Al_8$ MGs was investigated. The results showed that the contributing volume in the some polyhedra increases, the contributing volume of other polyhedra has a decreasing trend. Based on the differences of the contributing volume of polyhedra, the microstructural heterogeneity of MGs is revealed. By further identifying the volume expansion and contraction around each atom, the microstructural heterogeneity of MGs can be quantified. Through the Pearson correlation coefficient K , there is a linear relationship between the change ratio of polyhedral volume C_i and the number of quasi-nearest atoms N_Q . Dynamic mechanical tests performed in MD simulations showed that the $\langle C_i \rangle$ has a strong correlation with the normalized storage modulus E'/Eu and normalized loss modulus E''/Eu . Through adjusting the distribution of $\langle C_i \rangle$, dynamic heterogeneities in MGs can be changed. The present analysis offers a new perspective for understanding the evolution of microstructural heterogeneity of MGs quantitatively.

Acknowledgments

We thank Shao-Peng Pan from Taiyuan University of Technology for helpful discussion. This work was supported by 2017 Hong Kong Scholars Program and the Faculty of Engineering of The Hong Kong Polytechnic University under the account

no. 1-45-37-99QP.

References

- [1] Y.Q. Cheng, E. Ma. Atomic-level structure and structure-property relationship in metallic glasses. *Prog. Mater. Sci.*, 56 (2011) 379-473.
- [2] T.C. Hufnagel, C.A. Schuh, M.L. Falk. Deformation of metallic glasses: Recent developments in theory, simulations, and experiments. *Acta Mater.*, 109 (2016) 375-393.
- [3] J.R. Greer, J.T.M. De Hosson. Plasticity in small-sized metallic systems: Intrinsic versus extrinsic size effect. *Prog. Mater. Sci.*, 56 (2011) 654-724.
- [4] H.B. Lu, L.C. Zhang, A. Gebert, L. Schultz. Pitting corrosion of Cu-Zr metallic glasses in hydrochloric acid solutions. *J. Alloys Compd.*, 462 (2008) 60-67.
- [5] A. Gebert, P. Gostin, M. Uhlemann, J. Eckert, L. Schultz. Interactions between mechanically generated defects and corrosion phenomena of Zr-based bulk metallic glasses. *Acta Mater.*, 60 (2012) 2300-2309.
- [6] T. Egami. Mechanical failure and glass transition in metallic glasses. *J. Alloys Compd.*, 509 (2011) S82-S86.
- [7] J.C. Qiao, J.M. Pelletier. Analysis of atomic mobility in a $\text{Cu}_{38}\text{Zr}_{46}\text{Ag}_8\text{Al}_8$ bulk metallic glass. *J. Alloys Compd.*, 549 (2013) 370-374.
- [8] T. Ichitsubo, E. Matsubara, T. Yamamoto, H. Chen, N. Nishiyama, J. Saida, K. Anazawa. Microstructure of fragile metallic glasses inferred from ultrasound-accelerated crystallization in Pd-based metallic glasses. *Phys. Rev. Lett.*, 95 (2005) 245501.
- [9] A. Hirata, P. Guan, T. Fujita, Y. Hirotsu, A. Inoue, A.R. Yavari, T. Sakurai, M. Chen. Direct observation of local atomic order in a metallic glass. *Nat. Mater.*, 10 (2011) 28-33.
- [10] M. Zhang, L.H. Dai, Y. Liu, L. Liu. Heterogeneous dynamics of metallic glasses. *Scripta Mater.*, 107 (2015) 111-114.
- [11] W.L. Johnson, M.D. Demetriou, J.S. Harmon, M.L. Lind, K. Samwer. Rheology and ultrasonic properties of metallic glass-forming liquids: A potential energy landscape perspective. *MRS Bull.*, 32 (2007) 644-650.
- [12] E. Ma. Tuning order in disorder. *Nat. Mater.*, 14 (2015) 547-552.
- [13] M.H. Cohen, D. Turnbull. Molecular transport in liquids and glasses. *J. Chem. Phys.*, 31 (1959) 1164-1169.
- [14] F. Spaepen. A microscopic mechanism for steady state inhomogeneous flow in metallic glasses. *Acta Metall.*, 25 (1977) 407-415.
- [15] A.S. Argon. Plastic deformation in metallic glasses. *Acta Metall.*, 27 (1979) 47-58.
- [16] J. Sietsma, B.J. Thijsse. Characterization of free volume in atomic models of metallic glasses. *Phys. Rev. B*, 52 (1995) 3248-3255.
- [17] Y. Wang, M. Li, J. Xu. Toughen and harden metallic glass through designing statistical heterogeneity. *Scripta Mater.*, 113 (2016) 10-13.
- [18] Y. Wang, M. Li, J. Xu. Free volume gradient effect on mechanical properties of metallic glasses. *Scripta Mater.*, 130 (2017) 12-16.
- [19] Y. Wang, M. Li, J. Xu. Mechanical properties of spinodal decomposed metallic glass composites. *Scripta Mater.*, 135 (2017) 41-45.
- [20] J. Ding, Y.Q. Cheng, H. Sheng, M. Asta, R.O. Ritchie, E. Ma. Universal structural parameter to quantitatively predict metallic glass properties. *Nat. Commun.*, 7 (2016) 13733.
- [21] Q.K. Li, M. Li. Molecular dynamics simulation of intrinsic and extrinsic mechanical

- properties of amorphous metals. *Intermetallics*, 14 (2006) 1005-1010.
- [22] H.B. Yu, J. Hu, X.X. Xia, B.A. Sun, X.X. Li, W.H. Wang, H.Y. Bai. Stress-induced structural inhomogeneity and plasticity of bulk metallic glasses. *Scripta Mater.*, 61 (2009) 640-643.
- [23] L.Y. Chen, A.D. Setyawan, H. Kato, A. Inoue, G.Q. Zhang, J. Saida, X.D. Wang, Q.P. Cao, J.Z. Jiang. Free-volume-induced enhancement of plasticity in a monolithic bulk metallic glass at room temperature. *Scripta Mater.*, 59 (2008) 75-78.
- [24] G.J. Yang, B. Xu, L.T. Kong, J.F. Li, S. Zhao. Size effects in $\text{Cu}_{50}\text{Zr}_{50}$ metallic glass films revealed by molecular dynamics simulations. *J. Alloys Compd.*, 688 (2016) 88-95.
- [25] T. Egami. Understanding the properties and structure of metallic glasses at the atomic level. *JOM*, 62 (2010) 70-75.
- [26] Y.Q. Cheng, E. Ma. Indicators of internal structural states for metallic glasses: Local order, free volume, and configurational potential energy. *Appl. Phys. Lett.*, 93 (2008) 051910.
- [27] Q.K. Li, M. Li. Atomistic simulations of correlations between volumetric change and shear softening in amorphous metals. *Phys. Rev. B*, 75 (2007) 094101.
- [28] A.V. Granato. Interstitialcy model for condensed matter states of face-centered-cubic metals. *Phys. Rev. Lett.*, 68 (1992) 974-977.
- [29] A.V. Granato. Interstitialcy theory of simple condensed matter. *Eur. Phys. J. B*, 87 (2014) 18.
- [30] J. Perez, J. Cavaille, S. Etienne, F. Fouquet, F. Guyot. Internal friction in vitreous solid to glass transition. *Ann. Phys.*, 8 (1983) 417-467.
- [31] J.C. Qiao, Y. Yao, J.M. Pelletier, L.M. Keer. Understanding of micro-alloying on plasticity in $\text{Cu}_{46}\text{Zr}_{47-x}\text{Al}_7\text{Dy}_x$ ($0 \leq x \leq 8$) bulk metallic glasses under compression: Based on mechanical relaxations and theoretical analysis. *Int. J. Plast.*, 82 (2016) 62-75.
- [32] J.C. Qiao, Y.J. Wang, J.M. Pelletier, L.M. Keer, M.E. Fine, Y. Yao. Characteristics of stress relaxation kinetics of $\text{La}_{60}\text{Ni}_{15}\text{Al}_{25}$ bulk metallic glass. *Acta Mater.*, 98 (2015) 43-50.
- [33] Y.H. Liu, G. Wang, R.J. Wang, M.X. Pan, W.H. Wang. Super plastic bulk metallic glasses at room temperature. *Science*, 315 (2007) 1385-1388.
- [34] P. Donovan, R. Cochrane. Deformation-induced microcracking in $\text{Pd}_{40}\text{Ni}_{40}\text{P}_{20}$ metallic glass. *Scripta Metall.*, 22 (1988) 1765-1770.
- [35] K.M. Flores, D. Suh, R. Howell, P. Asoka-Kumar, P.A. Sterne, R.H. Dauskardt. Flow and fracture of bulk metallic glass alloys and their composites. *Mater. Trans.*, 42 (2001) 619-622.
- [36] Y. Xu, J. Fang, H. Gleiter, H. Hahn, J. Li. Quantitative determination of free volume in $\text{Pd}_{40}\text{Ni}_{40}\text{P}_{20}$ bulk metallic glass. *Scripta Mater.*, 62 (2010) 674-677.
- [37] D.Z. Chen, D. Jang, K.M. Guan, Q. An, W.A. Goddard, 3rd, J.R. Greer. Nanometallic glasses: size reduction brings ductility, surface state drives its extent. *Nano Lett.*, 13 (2013) 4462-4468.
- [38] D.Z. Chen, X.W. Gu, Q. An, W.A. Goddard, J.R. Greer. Ductility and work hardening in nano-sized metallic glasses. *Appl. Phys. Lett.*, 106 (2015) 061903.
- [39] G. Kumar, T. Ohkubo, T. Mukai, K. Hono. Plasticity and microstructure of Zr-Cu-Al bulk metallic glasses. *Scripta Mater.*, 57 (2007) 173-176.
- [40] N. Medvedev. The algorithm for three-dimensional Voronoi polyhedra. *J. Comput. Phys.*, 67 (1986) 223-229.
- [41] Y.Q. Cheng, E. Ma, H.W. Sheng. Atomic level structure in multicomponent bulk metallic glass. *Phys. Rev. Lett.*, 102 (2009) 245501.
- [42] S. Plimpton. Fast parallel algorithms for short-range molecular dynamics. *J. Comput. Phys.*, 117 (1995) 1-19.

- [43] H.B. Yu, K. Samwer. Atomic mechanism of internal friction in a model metallic glass. *Phys. Rev. B*, 90 (2014) 144201.
- [44] Q.K. Li, M. Li. Free volume evolution in metallic glasses subjected to mechanical deformation. *Mater. Trans.*, 48 (2007) 1816-1821.
- [45] S.D. Feng, L. Qi, L.M. Wang, S.P. Pan, M.Z. Ma, X.Y. Zhang, G. Li, R.P. Liu. Atomic structure of shear bands in $\text{Cu}_{64}\text{Zr}_{36}$ metallic glasses studied by molecular dynamics simulations. *Acta Mater.*, 95 (2015) 236-243.
- [46] S.D. Feng, K.C. Chan, S.H. Chen, L. Zhao, R.P. Liu. The role of configurational disorder on plastic and dynamic deformation in $\text{Cu}_{64}\text{Zr}_{36}$ metallic glasses: A molecular dynamics analysis. *Sci. Rep.*, 7 (2017) 40969.
- [47] S.P. Pan, S.D. Feng, J.W. Qiao, W.M. Wang, J.Y. Qin. Correlation between local structure and dynamic heterogeneity in a metallic glass-forming liquid. *J. Alloys Compd.*, 664 (2016) 65-70.
- [48] Y. Fan, T. Iwashita, T. Egami. How thermally activated deformation starts in metallic glass. *Nat Commun*, 5 (2014) 5083.
- [49] J.C. Qiao, Y.-J. Wang, L.Z. Zhao, L.H. Dai, D. Crespo, J.M. Pelletier, L.M. Keer, Y. Yao. Transition from stress-driven to thermally activated stress relaxation in metallic glasses. *Phys. Rev. B*, 94 (2016).
- [50] H.B. Yu, W.H. Wang, K. Samwer. The β relaxation in metallic glasses: an overview. *Mater. Today*, 16 (2013) 183-191.
- [51] J.C. Qiao, J.M. Pelletier. Dynamic mechanical relaxation in bulk metallic glasses: a review. *J. Mater. Sci. Technol.*, 30 (2014) 523-545.
- [52] J.C. Qiao, J.M. Pelletier. Influence of thermal treatments and plastic deformation on the atomic mobility in $\text{Zr}_{50.7}\text{Cu}_{28}\text{Ni}_9\text{Al}_{12.3}$ bulk metallic glass. *J. Alloys Compd.*, 615 (2014) S85-S89.
- [53] J.C. Qiao, J.M. Pelletier, C. Esnouf, Y. Liu, H. Kato. Impact of the structural state on the mechanical properties in a Zr-Co-Al bulk metallic glass. *J. Alloys Compd.*, 607 (2014) 139-149.

Figure Captions

Fig. 1 The distributions of the contributing volume of (a) Zr-centered, (b) Cu-centered and (c) Al-centered polyhedra with reheating at 550 K, 650 K and 750 K.

Fig. 2 Schematic description of the polyhedral volume distribution of models (a) as quenched and (b) reheated at 650 K. Atoms A and A' correspond to the volume expansion, while atoms B and B' correspond to the volume contraction.

Fig. 3 Volume parameter of C_i for (a) the model reheated from 450 K to 500 K and (b) the model reheated from 700 K to 750 K.

Fig. 4 (a) $\langle C_i \rangle$ as a function of $\langle N_Q \rangle$ with $n_a = 200$ for Zr, Cu and Al. For each element, the atoms are sorted by their $\langle N_Q \rangle$ from low to high. They are divided into n_g groups, each containing n_a atoms. For each group, the average C_i ($\langle C_i \rangle$) and N_Q ($\langle N_Q \rangle$) are calculated. (b) Pearson correlation coefficient as a function of n_a between $\langle N_Q \rangle$ and $\langle C_i \rangle$.

Fig. 5. Evolution of normalized storage modulus E'/E_u and normalized loss modulus E''/E_u as functions of $\langle C_i \rangle$ for Al centered polyhedra at different temperatures. Here, E_u is the non-relaxed modulus, which is assumed to be E' at 100 K.

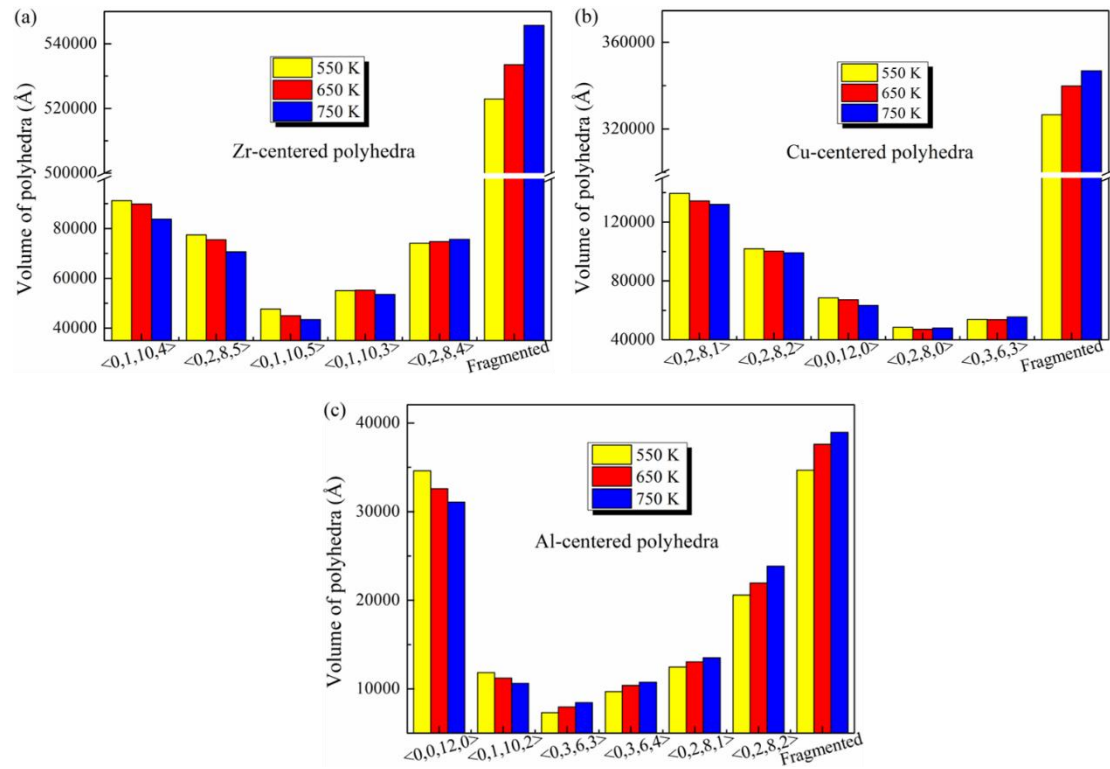


Fig. 1 The distributions of the contributing volume of (a) Zr-centered, (b) Cu-centered and (c) Al-centered polyhedra with reheating at 550 K, 650 K and 750 K.

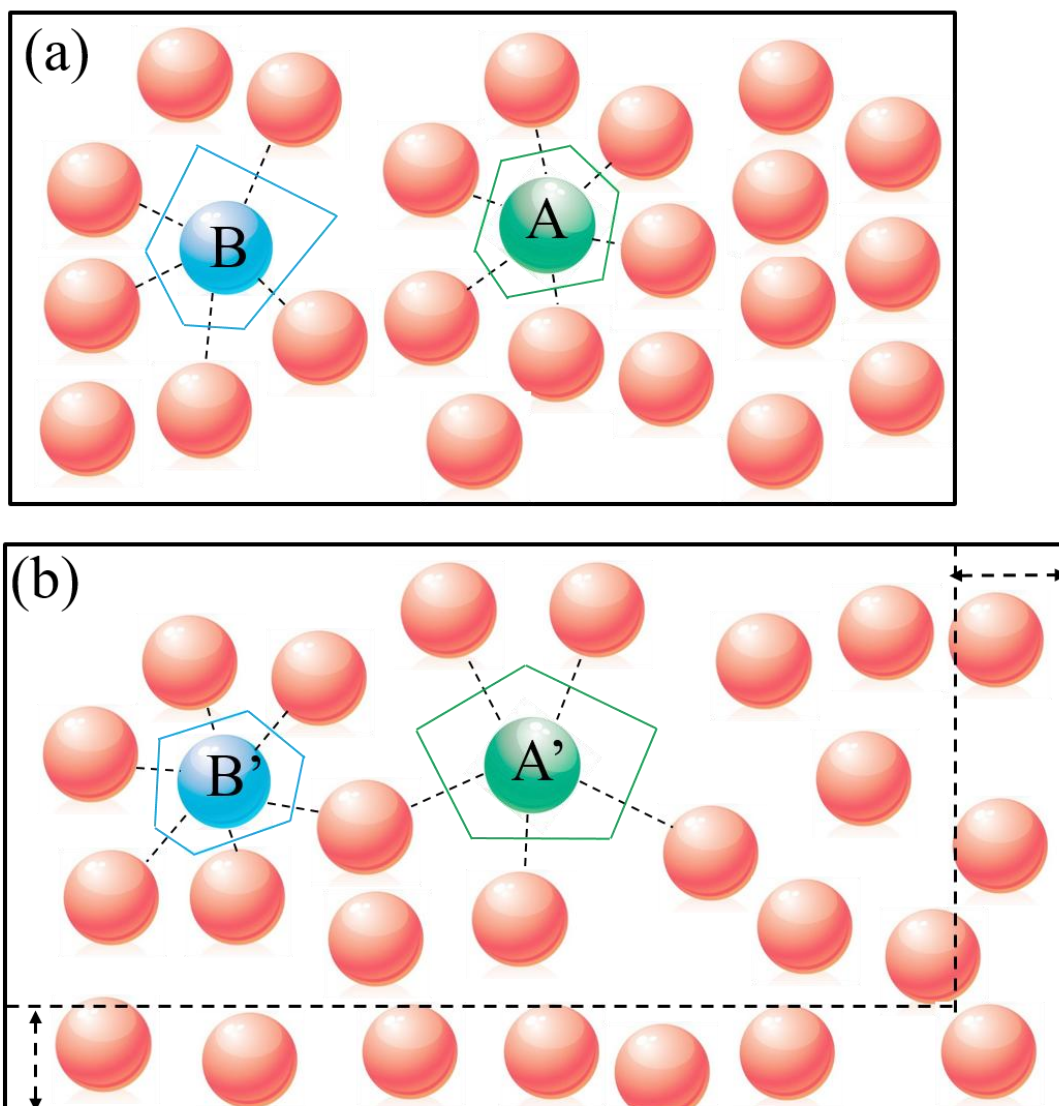


Fig. 2 Schematic description of the polyhedral volume distribution of models (a) as quenched and (b) reheated at 650 K. Atoms A and A' correspond to the volume expansion, while atoms B and B' correspond to the volume contraction.

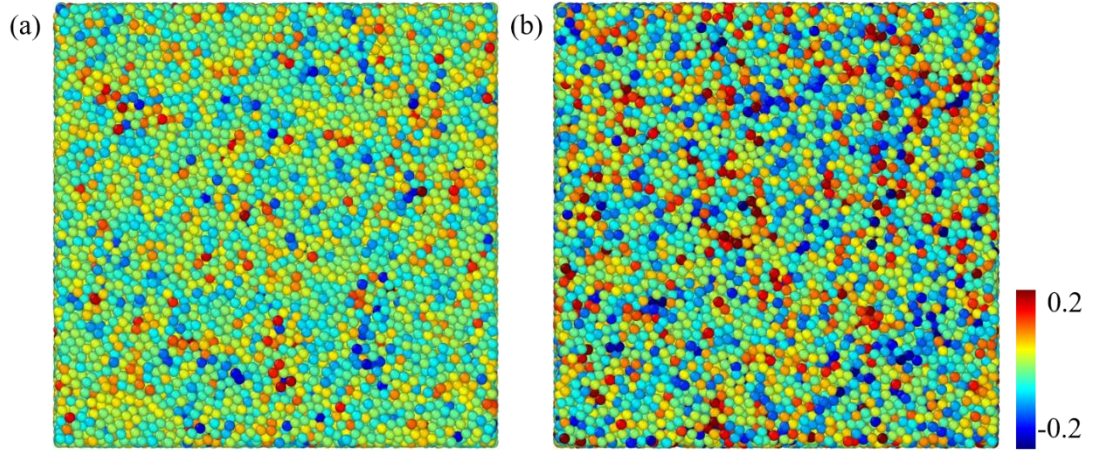


Fig. 3 Volume parameter of C_i for (a) the model reheated from 450 K to 500 K and (b) the model reheated from 700 K to 750 K.

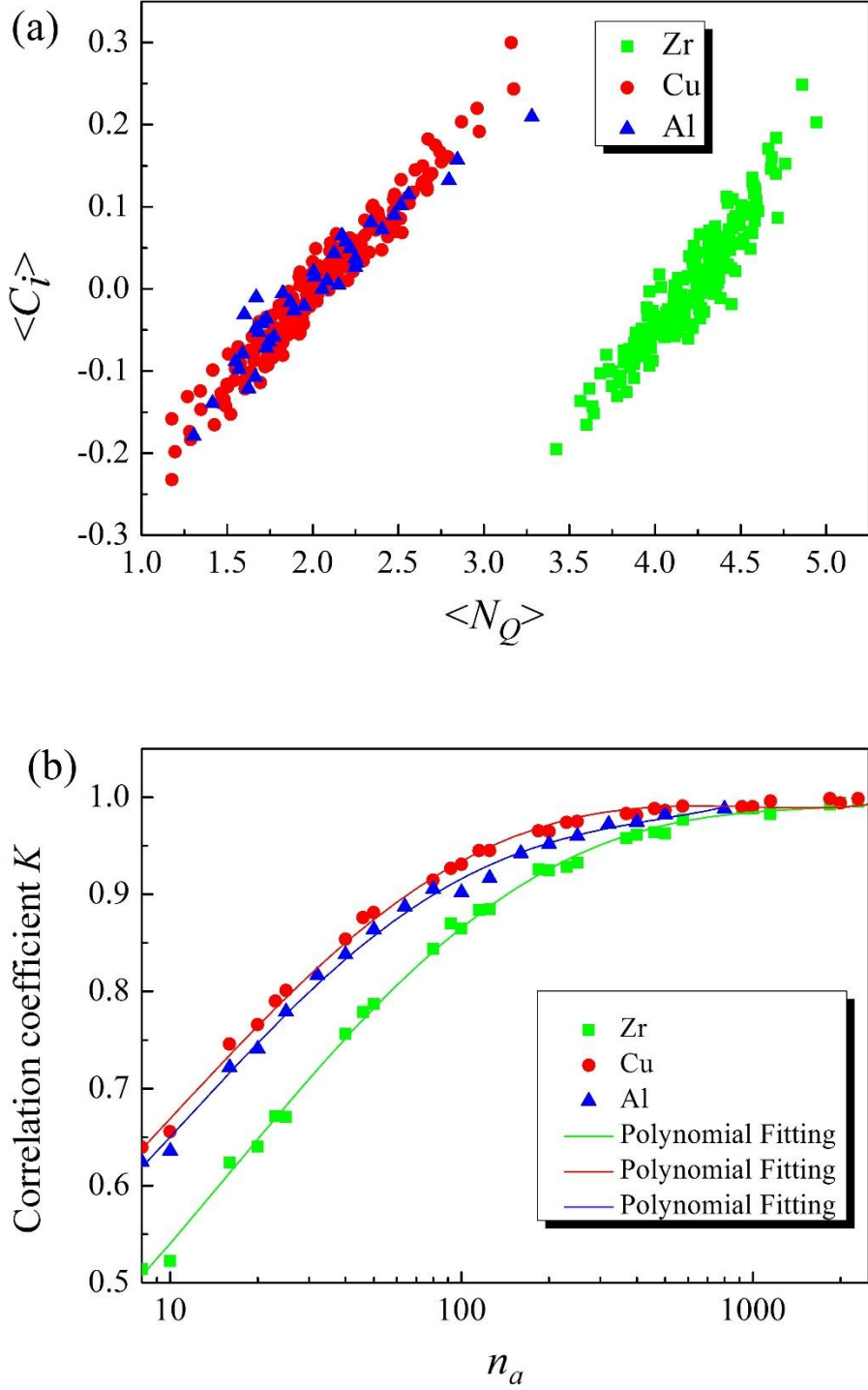


Fig. 4 (a) $\langle C_i \rangle$ as a function of $\langle N_Q \rangle$ with $n_a = 200$ for Zr, Cu and Al. For each element, the atoms are sorted by their $\langle N_Q \rangle$ from low to high. They are divided into n_g groups, each containing n_a atoms. For each group, the average C_i ($\langle C_i \rangle$) and N_Q ($\langle N_Q \rangle$) are calculated. (b) Pearson correlation coefficient as a function of n_a between $\langle N_Q \rangle$ and $\langle C_i \rangle$.

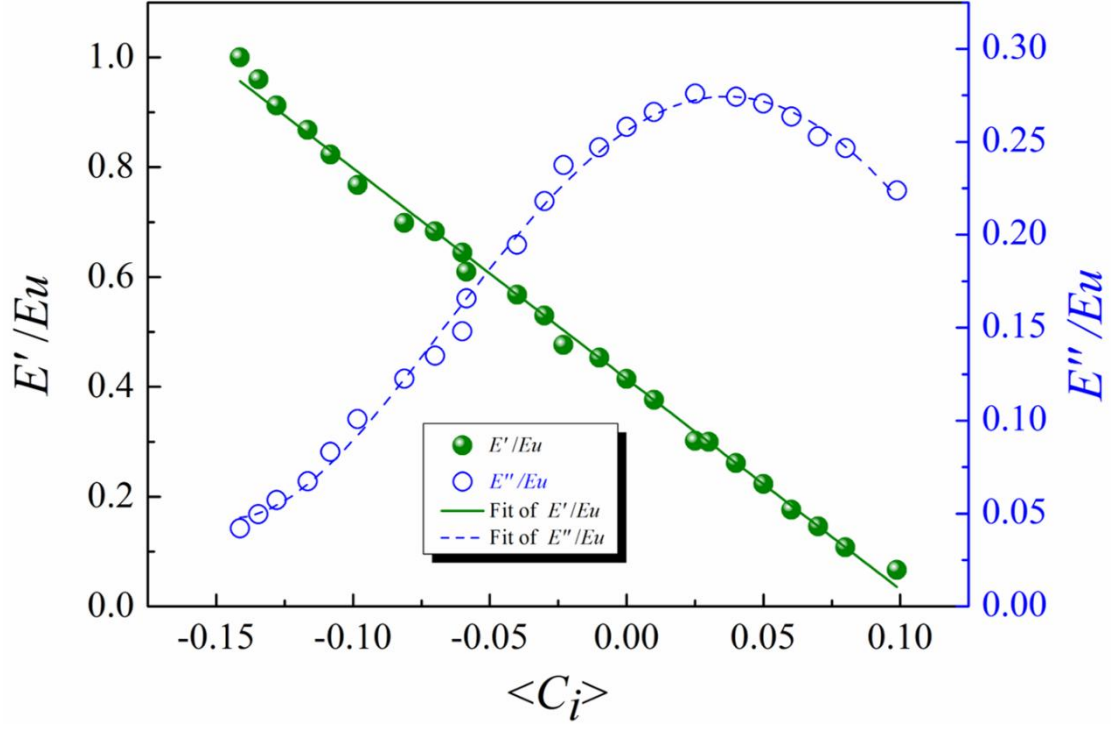
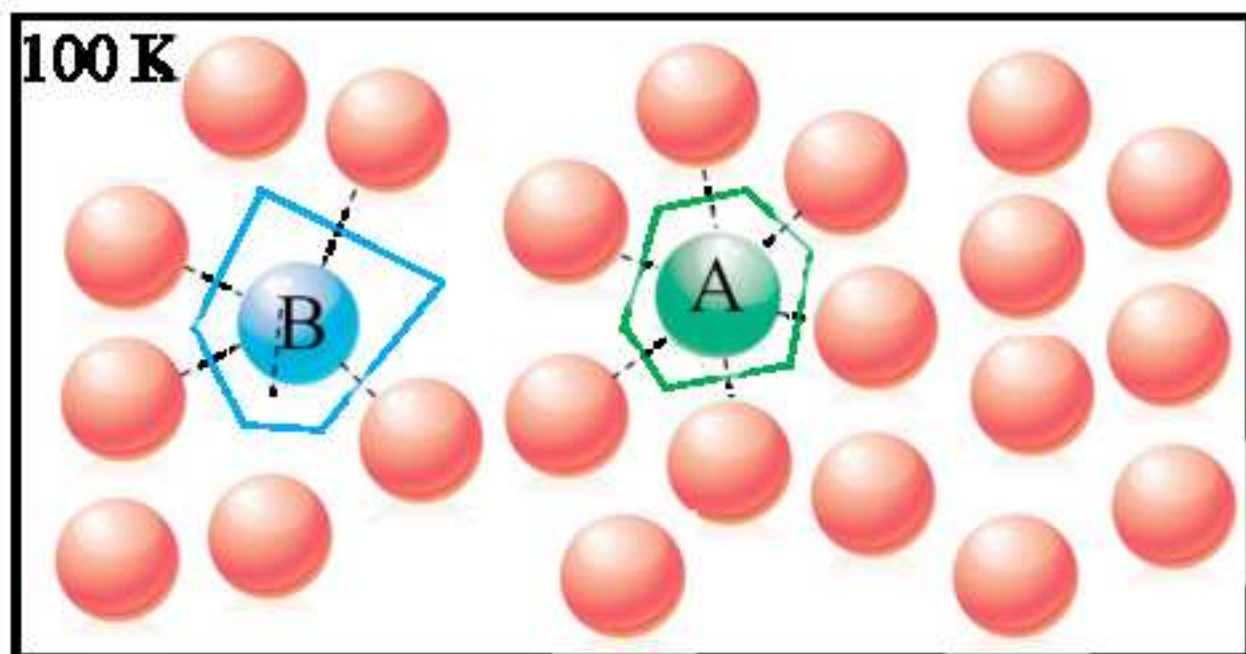
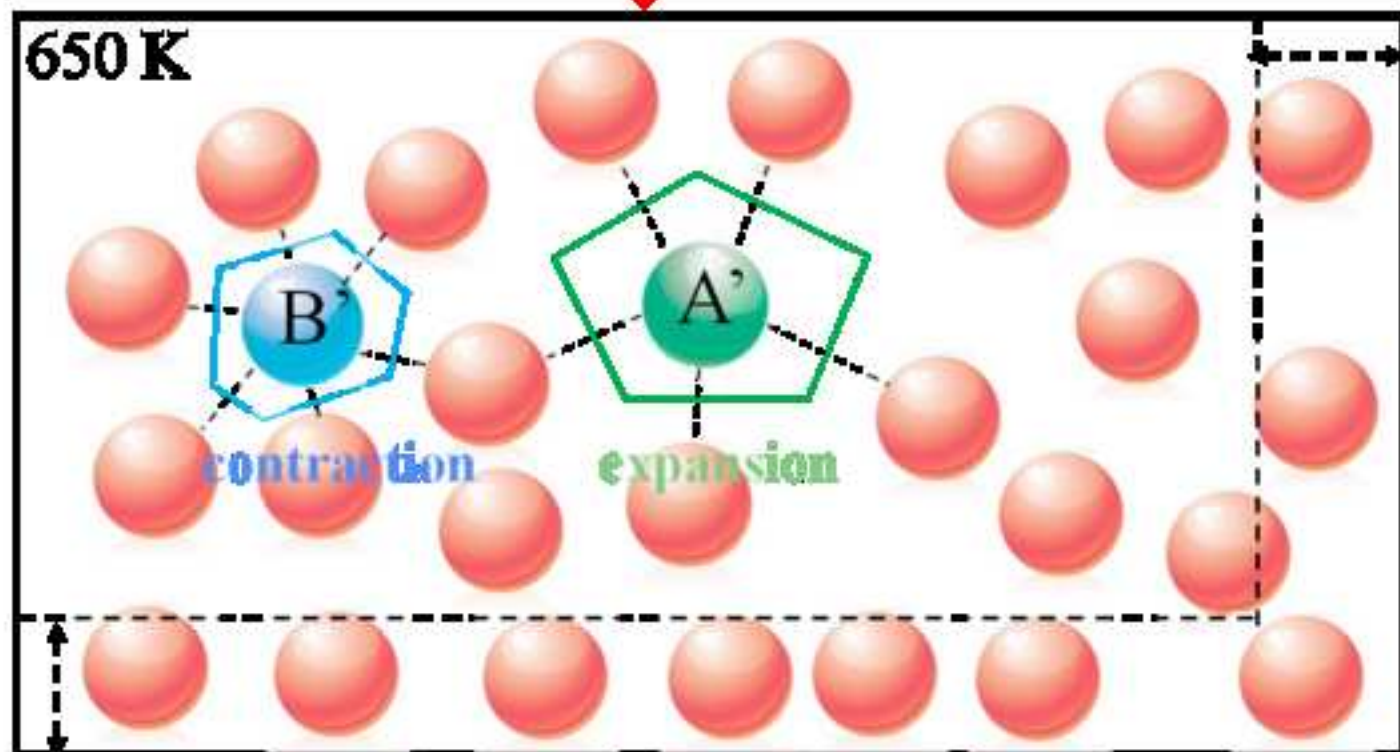


Fig. 5. Evolution of normalized storage modulus E'/E_u and normalized loss modulus E''/E_u as functions of $\langle C_i \rangle$ for Al centered polyhedra at different temperatures. Here, E_u is the non-relaxed modulus, which is assumed to be E' at 100 K.



Reheat  **Quantify heterogeneity**





THE HONG KONG
POLYTECHNIC UNIVERSITY

Advanced Manufacturing Technology Research Centre,
Department of Industrial and Systems Engineering

Prof. K.C.Chan.
Yuk Choi Road, Hung Hom
Kowloon, Hong Kong
Tel: (852) 2766 4981
Fax (852) 2362 5267
Email: kc.chan@polyu.edu.hk

Highlight:

- 1 The microheterogeneity is characterized by polyhedral volumes quantitatively.
- 2 The simulations allow reproduction of evolutions of atomic-level heterogeneity.
- 3 The simulation results are in good agreement with experiments and theories.
- 4 The heterogeneities can be predicted by the distributions of polyhedral volumes.